Effects of Hydrogen Bonding in Electron-Transfer Reactions of $[Co(en)_3]^{2+}$

Robert M. L. Warren, Akira Tatehata,[1] and A. Graham Lappin*

Department of Chemistry and Biochemistry, University of Notre Dame, Notre Dame, Indiana 46556

Received October 8, 1992

The kinetics and mechanisms of the reductions of the complexes $[Co(gly)(ox)_2]^{2-}$, $[Co(edta)]^-$, *cis*-α-$[Co(edda)(ox)]^-$, *cis*-β-$[Co(edda)(ox)]^-$, C_1-*cis*(*N*)-$[Co(gly)_2(ox)]^-$, C_2-*cis*(*N*)-$[Co(gly)_2(ox)]^-$, *trans*(*N*)-$[Co(gly)_2(ox)]^-$, $[Co(en)(ox)_2]^-$, and $[Co(en)_2(ox)]^+$ by $[Cr(bpy)_3]^{2+}$, $[Co(en)_3]^{2+}$, and $[Co(en)_2]^{2+}$ have been examined in aqueous solution. Reactions with $[Cr(bpy)_3]^{2+}$ are outer-sphere in nature and have rate constants in the range (1–200) × 10^4 M^{-1} s^{-1} at 25.0 °C and 0.10 M ionic strength. Reactions with $[Co(en)_3]^{2+}$ are also outer-sphere with rate constants in the range (1–20 000) × 10^{-3} M^{-1} s^{-1} at 25.0 °C and 0.10 M ionic strength. The rates for reactions of the anionic complexes follow two distinct linear free-energy correlations with those of $[Cr(bpy)_3]^{2+}$. Free energies of activation for reactions of $[Co(en)_3]^{2+}$ with the complexes $[Co(edta)]^-$, *cis*-β-$[Co(edda)(ox)]^-$ and C_1-*cis*(*N*)-$[Co(gly)_2(ox)]^-$ are 4 kJ mol^{-1} lower than predicted from the reactions with the other anionic species *cis*-α-$[Co(edda)(ox)]^-$, C_2-*cis*(*N*)-$[Co(gly)_2(ox)]^-$, *trans*(*N*)-$[Co(gly)_2(ox)]^-$, and $[Co(en)(ox)_2]^-$. This is ascribed to the presence of an unhindered pseudo-C_3 carboxylate motif which enhances hydrogen bonding in ion pairing with $[Co(en)_3]^{2+}$. Further evidence for this distinction has been obtained from stereoselectivity studies. In reactions of the optically active oxidants, the Δ isomers yield $[Co(en)_3]^{3+}$ which has an enantiomeric excess around 10% of the Λ form when the pseudo-C_3 motif is present and around 2% of the Λ form when it is not. The effect of the paramagnetic probe $[Cr(en)_3]^{3+}$ on the ^1H NMR relaxation rates of *cis*-α-$[Co(edda)(ox)]^-$ and *cis*-β-$[Co(edda)(ox)]^-$ also reveals that the ion-pairing interactions differ for the two sets of oxidants. Reactions of $[Co(en)_2]^{2+}$ with the oxalato complexes are inner-sphere and are faster by an order of magnitude than the corresponding reactions with $[Co(en)_3]^{2+}$. Stereoselectivity is observed and is determined by the nature of the ligand donor atoms cis to both arms of the bridging oxalate group.

Introduction

Outer-sphere electron-transfer reactions of $[Co(en)_3]^{2+}$ (en = 1,2-diaminoethane) with a number of anionic cobalt(III) oxidants have been the subject of recent detailed investigations featuring the use of chiral induction as a mechanistic probe.[2-5] With $[Co(edta)]^-$, $[Co(ox)_3]^{3-}$, and $[Co(mal)_3]^{3-}$ (edta = 1,2-diaminoethane-*N*,*N*,*N*′,*N*′-tetraacetate(4–), ox = oxalate(2–), mal = malonate(2–)) the Δ form of the oxidant invariably yields a modest enantiomeric excess, ≤10%, of the Λ-$[Co(en)_3]^{3+}$ product. Extension of these studies to include $[Co(gly)(ox)_2]^{2-}$, $[Co(en)(ox)_2]^-$, and the three isomers of $[Co(gly)_2(ox)]^-$ (gly = glycinate(1–)) confirm that this $\Delta\Lambda$ preference is found for all anionic complexes;[6,7] however, the magnitude of the induction is distinctly dependent on whether or not the oxidant has a C_3 axis (or pseudo-C_3 axis) featuring three sterically unhindered carboxylate groups, Figure 1. Where this motif exists, the stereoselectivities are higher, ≈7–10% enantiomeric excess, but where these groups are hindered by the ligand backbone, much more modest stereoselectivities, ≈2–3%, are observed. It has been suggested that enhanced stereoselectivity is the result of the increased opportunity for hydrogen bonding with amine hydrogens on the C_3 face of $[Co(en)_3]^{2+}$ afforded by the unhindered carboxylate groups. The two classes of reactivity are further defined when comparisons are made with ion-pairs formed between the oxidants and $[Co(en)_3]^{3+}$, which serves as an analogue for $[Co(en)_3]^{2+}$. Not only are the ion-pairing constants much larger when the pseudo-C_3 axis is unhindered, but they are also in the same sense, with a $\Delta\Lambda$ preference, as the chiral induction in the electron transfer.[8-11] When the axis is hindered, the ion pairing preference is $\Delta\Delta$.

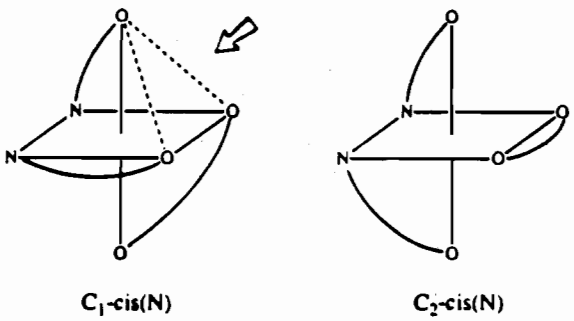

Figure 1. Structures of C_1-*cis*(*N*)-$[Co(gly)_2(ox)]^-$ (showing the unhindered pseudo-C_3 axis) and C_2-*cis*(*N*)-$[Co(gly)_2(ox)]^-$.

An objective of the present study is to discover what effects these differences in hydrogen-bonding structure reveal in the kinetics of the stereoselective electron-transfer reactions in aqueous solution. Accordingly, the kinetics and mechanisms of reductions of the complexes $[Co(gly)(ox)_2]^{2-}$, $[Co(edda)(ox)]^-$, $[Co(gly)_2(ox)]^-$, and $[Co(en)(ox)_2]^-$ with $[Co(en)_3]^{2+}$ (edda = 1,2-diaminoethane-*N*,*N*′-diacetate(2–)) have been examined. The corresponding reductions by $[Cr(bpy)_3]^{2+}$ (bpy = 2,2′-bipyridine) allow comparisons with an outer-sphere reaction in which hydrogen bonding plays no direct role. In addition to the outer-sphere pathway, oxalate has been shown to form an effective bridge for inner-sphere electron transfer in the reduction of $[Co(ox)_3]^{3-}$ by $[Co(en)_3]^{2+}$.[4] The resulting product, $[Co(en)_2(ox)]^+$, is formed stereoselectively. The presence of oxalate as a potential bridging ligand in the complexes $[Co(gly)(ox)_2]^{2-}$,

(1) Visiting Professor from the Department of Chemistry, Faculty of Science, Shizuoka University, Ohya, Shizuoka 422, Japan.
(2) Geselowitz, D. A.; Taube, H. *J. Am. Chem. Soc.* **1980**, *102*, 4525–4526.
(3) Osvath, P.; Lappin, A. G. *Inorg. Chem.* **1987**, *26*, 195–202.
(4) Marusak, R. A.; Osvath, P.; Kemper, M.; Lappin, A. G. *Inorg. Chem.* **1989**, *28*, 1542–1548.
(5) Geselowitz, D. A.; Hammershøi, A.; Taube, H. *Inorg. Chem.* **1987**, *26*, 1842–1845.
(6) Tatehata, A.; Mitani, T. *Chem. Lett.* **1989**, 1167–1170.
(7) Tatehata, A.; Akita, H. *Bull. Chem. Soc. Jpn.* **1991**, *64*, 1985–1987.
(8) Tatehata, A.; Iiyoshi, M.; Kotsuji, K. *J. Am. Chem. Soc.* **1981**, *103*, 7391–7392.
(9) Tatehata, A.; Fujita, M.; Ando, K.; Asaba, Y. *J. Chem. Soc., Dalton Trans.* **1987**, 1977–1982.
(10) Tatehata, A.; Asaba, Y. *Bull. Chem. Soc. Jpn.* **1988**, *61*, 3145–3151.
(11) Miyoshi, K.; Sakamoto, Y.; Ohguni, A.; Yoneda, H. *Bull. Chem. Soc. Jpn.* **1985**, *58*, 2239–2246.

0020-1669/93/1332-1191$04.00/0

$[Co(edda)(ox)]^-$, $[Co(gly)_2(ox)]^-$, and $[Co(en)(ox)_2]^-$ provides an opportunity for systematic study of inner-sphere stereoselectivity.

Experimental Section

(a) Materials. $Na[Co(en)(ox)_2]\cdot H_2O$ was prepared by the method of Dwyer, in yields much lower than reported.[12] $Na(\Delta\text{-}(+)_{546}\text{-}[Co(en)(ox)_2])\cdot 3.5H_2O$ ($\epsilon_{541} = 109\ M^{-1}\ cm^{-1}$; $\Delta\epsilon_{581} = -2.53\ M^{-1}\ cm^{-1}$)[13] was resolved with use of $(+)_{546}\text{-}[Co(en)_2(NO_2)_2]Br$.[14] $Ba[Co(gly)(ox)_2]\cdot 0.5H_2O$ was prepared[15] and converted to $Na_2[Co(gly)(ox)_2]\cdot 1.5H_2O$ with Na_2SO_4. $Ba(\Delta\text{-}(+)_{546}\text{-}[Co(gly)(ox)_2])\cdot 2.5H_2O$ was resolved with use of $\Lambda\text{-}(+)_{589}\text{-}[Co(en)_2(ox)]I$ and converted with Na_2SO_4 to the more soluble $Na_2(\Delta\text{-}(+)_{546}\text{-}[Co(gly)(ox)_2])\cdot H_2O$ ($\epsilon_{565} = 138\ M^{-1}\ cm^{-1}$; $\Delta\epsilon_{581} = -3.08\ M^{-1}\ cm^{-1}$). $[Co(en)_2(ox)]Cl\cdot H_2O$,[16] $\Lambda\text{-}(+)_{589}\text{-}[Co(en)_2(ox)]I$ ($\epsilon_{500} = 103\ M^{-1}\ cm^{-1}$; $\Delta\epsilon_{520} = +2.64\ M^{-1}\ cm^{-1}$),[17,18] $Na[Co(edta)]\cdot 2H_2O$,[19] $Na(\Delta\text{-}(+)_{546}\text{-}[Co(edta)])\cdot 4H_2O$ ($\epsilon_{535} = 331\ M^{-1}\ cm^{-1}$; $\Delta\epsilon_{575} = -1.79\ M^{-1}\ cm^{-1}$),[20] and $[Cr(en)_3]Cl_3\cdot 3.5H_2O$[21] were prepared as described previously.

The geometric isomers[22] *C_1-cis(N)*-$[Co(gly)_2(ox)]^-$, *C_2-cis(N)*-$[Co(gly)_2(ox)]^-$, and *trans(N)*-$[Co(gly)_2(ox)]^-$ were separated using a 45 × 3 cm diameter DEAE-Sephadex A-25 anion exchange column in the chloride form, with 0.25 M sodium chloride as an eluent. Resolution of the isomers was carried out as described in the literature,[23] using strychnine hemisulfate as resolving agent for the C_1-cis(N)- and C_2-cis(N) isomers and $\Lambda\text{-}(+)_{589}\text{-}[Co(en)_2(ox)]I$ for the trans(N) isomer. The absolute configurations are $K(\Delta\text{-}(-)_{546}\text{-}C_1\text{-}cis(N)\text{-}[Co(gly)_2(ox)])\cdot 0.5H_2O$ ($\epsilon_{546} = 141\ M^{-1}\ cm^{-1}$; $\Delta\epsilon_{565} = +2.48\ M^{-1}\ cm^{-1}$), $Na(\Delta\text{-}(-)_{546}\text{-}C_2\text{-}cis(N)\text{-}[Co(gly)_2(ox)])\cdot 2H_2O$ ($\epsilon_{561} = 120\ M^{-1}\ cm^{-1}$, $\Delta\epsilon_{555} = +3.39\ M^{-1}\ cm^{-1}$), and $Na(\Delta\text{-}(-)_{546}\text{-}trans(N)\text{-}[Co(gly)_2(ox)])$ ($\epsilon_{530} = 100\ M^{-1}\ cm^{-1}$; $\Delta\epsilon_{533} = +2.07\ M^{-1}\ cm^{-1}$). $Na(cis\text{-}\alpha\text{-}[Co(edda)(ox)])\cdot 2H_2O$ and $Na(cis\text{-}\beta\text{-}[Co(edda)(ox)])\cdot 2H_2O$ were prepared as described previously.[24] The two isomers were separated chromatographically on a 45 × 3 cm diameter DEAE-Sephadex A-25 anion exchange column in the chloride form, using 0.03 M $[Co(en)_3]Cl_3$ as an eluent. Resolution of the cis-α isomer[25] was achieved using $\Lambda\text{-}(+)_{589}\text{-}[Co(en)_2(ox)]I$ to yield $K(\Delta\text{-}cis\text{-}\alpha\text{-}[Co(edda)(ox)])\cdot 2H_2O$ ($\epsilon_{557} = 124\ M^{-1}\ cm^{-1}$; $\Delta\epsilon_{560} = -5.32\ M^{-1}\ cm^{-1}$). Preparation of $K(\Delta\text{-}(-)_{589}\text{-}cis\text{-}\beta\text{-}[Co(edda)(ox)])\cdot 2H_2O$ ($\epsilon_{528} = 215\ M^{-1}\ cm^{-1}$; $\Delta\epsilon_{540} = -2.19\ M^{-1}\ cm^{-1}$) was carried out by the literature method.[26] Anhydrous cobalt triflate (cobalt trifluoromethanesulfonate) $Co(CF_3SO_3)_2$ was prepared from $CoCO_3$ and CF_3SO_3H at 80–85 °C; the compound was filtered and dried by repeated recrystallization from methanol and evaporation under reduced pressure.

(b) Methods. The kinetics of reduction of the complexes by cobalt(II) in solutions of 1,2-diaminoethane were investigated under pseudo-first-order conditions using an excess of reductant at 0.10 M ionic strength (KNO_3 or KCl media). Typically oxidant concentrations were 2×10^{-4} M, with cobalt(II) concentrations in the range $(2–10) \times 10^{-3}$ M. The reactions were buffered by addition of small amounts of HCl or HNO_3 as appropriate, taking advantage of the first protonation of the 1,2-diaminoethane. Where quantitative (>99%) formation of the reductant $[Co(en)_3]^{2+}$ was desired, the [en] excess was typically 0.10 M.[27] For experiments in D_2O, anhydrous $Co(CF_3SO_3)_2$ was used as the source of cobalt(II).

All solutions were prepared immediately prior to use under an atmosphere of argon gas. The decrease in absorbance of the oxidant was monitored using a Varian Instruments Cary 3 spectrophotometer, equipped with a water-jacketed cell holder, giving temperature control to better than ±0.2 °C. Stopped-flow kinetics were monitored on a Durrum Model D-110 stopped-flow spectrophotometer, modified to enable solutions to be handled under an atmosphere of argon, and thermostated at 25.0 ± 0.1 °C. The pH was measured immediately after the reaction using a Beckman SelectIon 2000 meter, equipped with a Corning combination glass electrode with a saturated calomel (NaCl) reference. Plots of $\ln(A - A_\infty)$ against time were generally linear for at least 3 half-lives, and pseudo-first-order rate constants, k_{obsd}, were calculated from the slopes by least squares analysis. The pseudo-first-order rate constants are collected in Table SI, available as supplementary material.

The reductant $[Cr(bpy)_3]^{2+}$ was prepared[28] by reduction of a solution of $CrCl_3\cdot 6H_2O$ ($[Cr(H_2O)_6]^{3+}$: $\epsilon_{408} = 15.5\ M^{-1}\ cm^{-1}$; $\epsilon_{571} = 13.2\ M^{-1}\ cm^{-1}$)[29] over zinc amalgam and subsequent transfer to a 10^{-2} M solution of bipyridine. All solutions were prepared immediately prior to use under an atmosphere of argon gas. The kinetics of reduction of the complexes by $[Cr(bpy)_3]^{2+}$ were investigated under pseudo-first-order conditions using an excess of oxidant at 0.10 M ionic strength (KCl media). The reaction was monitored by observing the decrease in absorbance of the reductant at 467 nm on a Durrum Model D-110 stopped-flow spectrophotometer. Reductant concentrations were $(5–50) \times 10^{-6}$ M, with oxidant concentrations in the range $(5–100) \times 10^{-5}$ M. The reaction was buffered at pH 8.0 with 0.01 M tris(hydroxymethyl)aminomethane (Tris). The pH was measured immediately after the reaction, and pseudo-first-order rate constants were calculated as described above. The pseudo-first-order rate constants are collected in Table SII, available as supplementary material.

Stereoselectivity experiments at low 1,2-diaminoethane concentrations were carried out at 23.5 ± 1.0 °C in 0.1 M KNO_3 media. In a typical experiment 10 mL of a solution containing 4.30×10^{-2} M $Co(NO_3)_2$, 10 mL of a solution containing 4.30×10^{-2} M 1,2-diaminoethane, and 10 mL of a solution containing 4.30×10^{-3} M optically active oxidant were mixed under an atmosphere of argon. After 5 min the reactions were quenched with 2 mL of a degassed solution of 3 M HCl. The resulting solution was then diluted to 1 L and isolated on a 15 × 2.5 cm diameter SP-Sephadex C-25 cation exchange column. The column was washed with water, and the product, $[Co(en)_2(ox)]^+$, was eluted with 0.01 M HCl, evaporated to dryness under reduced pressure, and then made up to 25 mL in a volumetric flask. At higher [en], a similar procedure was used to isolate the $[Co(en)_3]^{3+}$ formed.[6] Reaction stoichiometries were measured by spectrophotometric determination of the reaction products. Circular dichroism spectra of the optically active products were run on an Aviv Model 60DS circular dichroism spectropolarimeter or a Jasco J-500 spectropolarimeter.

Stereoselectivity experiments in D_2O were carried out at 23.5 ● 1.0 °C in 0.1 M ionic strength (KCl) media. In a typical experiment 5 mL of a solution containing 0.10 M $Co(CF_3SO_3)_2$, 10 mL of a solution containing 0.5 M 1,2-diaminoethane, and 10 mL of a solution containing 5.00×10^{-3} M optically active oxidant were mixed under an atmosphere of argon. After complete disappearance of the color of the oxidant (5–10 min for *C_1-cis(N)*-$[Co(gly)_2(ox)]^-$; 30–45 min for *C_2-cis(N)*-$[Co(gly)_2(ox)]^-$), the reactions were quenched with 5 mL of a degassed solution of 3 M HCl. The product $[Co(en)_3]^{3+}$ was then isolated and characterized as described previously.[6]

^1H NMR spectra were accumulated on a Nicolet NT-300 MHz instrument at 25.0 ± 0.5 °C. T_1 determinations were carried out using an inversion-recovery program. This employs the usual 180°–τ–90° pulse sequence, where τ is the delay time. At least 11 different delay times were used in each experiment. Spin–lattice relaxation rates were evaluated by plotting $\ln(I_0 - I)$ against τ and calculating the slopes ($-1/T_1$) by least-squares analysis. All solutions for NMR studies were prepared with Cambridge Isotope Laboratories 99.9% D_2O under an atmosphere of argon gas to eliminate any effect of paramagnetic oxygen on the relaxation times.

(12) Dwyer, F. P.; Reid, I. K.; Garvan, F. L. *J. Am. Chem. Soc.* **1961**, *83*, 1285–1287.
(13) Douglas, B. E.; Haines, R. A.; Brushmiller, J. G. *Inorg. Chem.* **1963**, *2*, 1194–1198.
(14) Worrell, J. H. *Inorg. Synth.* **1972**, *13*, 195–202.
(15) Yamasaki, K.; Hidaka, J.; Shimura, Y. *Bull. Chem. Soc. Jpn.* **1969**, *42*, 119–126.
(16) Jordan, W. T.; Froebe, L. R.; Haines, R. A.; Leah, T. D. *Inorg. Synth.* **1978**, *18*, 96–102.
(17) Jordan, W. T.; Brennan, B. J.; Froebe, L. R.; Douglas, B. E. *Inorg. Chem.* **1973**, *12*, 1827–1831.
(18) McCaffery, A. J.; Mason, S. F.; Norman, B. J. *J. Chem. Soc.* **1965**, 5094–5107.
(19) Dwyer, F. P.; Gyarfas, E. C.; Mellor, D. J. *J. Phys. Chem.* **1955**, *59*, 296–297.
(20) Gillard, R. D.; Mitchell, P. R.; Weick, C. F. *J. Chem. Soc., Dalton Trans.* **1974**, 1635–1636.
(21) Gillard, R. D.; Mitchell, P. R.; Busch, D. H.; Sperati, C. R.; Jonassen, H. B.; Weston, C. W. *Inorg. Synth.* **1972**, *13*, 184–186.
(22) Matsuoka, N.; Hidaka, J.; Shimura, Y. *Bull. Chem. Soc. Jpn.* **1967**, *40*, 1868–1874.
(23) Matsuoka, N.; Hidaka, J.; Shimura, Y. *Inorg. Chem.* **1970**, *9*, 719–723.
(24) Coleman, P. F.; Legg, J. I.; Steele, J. *Inorg. Chem.* **1970**, *9*, 937–944.
(25) van Saun, C. W.; Douglas, B. E. *Inorg. Chem.* **1969**, *8*, 115–118.
(26) Jordan, W. T.; Legg, J. I. *Inorg. Chem.* **1974**, *13*, 955–959.
(27) Stability and acidity constants for $[Co(en)_3]^{2+}$ are $\log K_1 = 5.6$, $\log K_2 = 4.9$, $\log K_3 = 3.3$, $pK_{a1} = 7.08$, $pK_{a2} = 9.89$ at 25.0 °C and 0.10 M ionic strength: Smith, R. M.; Martell, A. E. *Critical Stability Constants*; Plenum: New York 1975; Vol. 2, p 36.
(28) Zwickel, A. M.; Taube, H. *Discuss. Faraday Soc.* **1960**, *29*, 42–48.
(29) Hyde, M. R.; Weighardt, K.; Sykes, A. G. *J. Chem. Soc., Dalton Trans.* **1976**, 690–694.

Table I. Percent Recovery of Oxidized Product for Reaction of a Series of Complexes with Cobalt(II) in Solutions of 1,2-Diaminoethane at 25.0 °C and 0.10 M Ionic Strength[a]

oxidant	% recovery of $[Co(en)_3]^{3+}$ [b]	% recovery of $[Co(en)_2(ox)]^+$ [c]
$[Co(ox)_3]^{3-}$	84(8),[d] 97(3)[e]	100(1)[d]
$[Co(gly)(ox)_2]^{2-}$	94(1)[e]	95(1)
[Co(edta)]	101(1)[e]	0
cis-β-[Co(edda)(ox)]⁻	94(1)	97(1)
C_1-*cis*(*N*)-$[Co(gly)_2(ox)]^-$	98(1),[e] 88(1)[f]	90(1)
cis-α-[Co(edda)(ox)]⁻	80(1)	95(1)
C_2-*cis*(*N*)-$[Co(gly)_2(ox)]^-$	71(1),[e] 79(1)[f]	92(1)
trans(*N*)-$[Co(gly)_2(ox)]^-$	77(4)[e]	92(1)
$[Co(en)(ox)_2]^-$	72(9)[e]	98(1)

[a] Percent recovery of oxidized product based on expected 1:1 reaction stoichiometry. Numbers in parentheses indicate error in the last significant figure(s). [b] Typical conditions were $[Co(II)] = 2.5 \times 10^{-2}$ M, [en] = 2.5 × 10^{-1} M, [oxidant] = 2.5×10^{-3} M, reaction time 5–10 min. [c] Typical conditions were $[Co(II)] = 1.43 \times 10^{-2}$ M, [en] = 1.43×10^{-2} M, [oxidant] = 1.43×10^{-3} M, reaction time 5 min. [d] Reference 4. [e] Reference 6. [f] In D_2O.

Table II. Second-Order Rate Constants for Reaction of a Series of Oxidants with $[Cr(bpy)_3]^{2+}$, $[Co(en)_3]^{2+}$, and $[Co(en)_2]^{2+}$ at 25.0 °C and 0.10 M Ionic Strength[a]

	reductant			
oxidant	$[Cr(bpy)_3]^{2+}$ $10^5 k_{Cr}$ (M^{-1} s^{-1})	$[Co(en)_3]^{2+}$ k_{os} (M^{-1} s^{-1})	$[Co(en)_2]^{2+}$ k_{is} (M^{-1} s^{-1})	10^5-k_{Cr}/k_{os}
$[Co(ox)_3]^{3-}$		390[b]	3300[b]	
$[Co(gly)(ox)_2]^{2-}$		20(1)	190(40)	
[Co(edta)]	20(1)[c]	18(3)[d]	*e*	1.1
cis-β-[Co(edda)(ox)]⁻	1.1(1)	0.87(2)	5(1)	1.3
C_1-*cis*(*N*)-$[Co(gly)_2(ox)]^-$	1.7(1)	1.50(2)	15(3)	1.1
cis-α-[Co(edda)(ox)]⁻	2.1(1)	0.37(1)	10(2)	5.7
C_2-*cis*(*N*)-$[Co(gly)_2(ox)]^-$	2.4(1)	0.44(1)	24(5)	5.5
trans(*N*)-$[Co(gly)_2(ox)]^-$	1.65(2)	0.28(1)	12(2)	5.9
$[Co(en)(ox)_2]^-$	0.85(2)	0.16(1)	9(2)	5.3
$[Co(en)_2(ox)]^+$	0.10(1)	0.0011(1)		
$[Co(en)_3]^{3+}$	3.7×10^{-4} [f]	3.2×10^{-5} [g]		

[a] Numbers in parentheses indicate error in the last significant figure(s). [b] 25.0 °C, 0.10 M $NaClO_4$ media, from ref 4. [c] Compare with 2.2×10^6 M^{-1} s^{-1} in 0.5 M NaCl media at 25.0 °C.[31] [d] Compare with 5.24 M^{-1} s^{-1} at 25.0 °C, I = 1.00 M, from ref 5 and 17 M^{-1} s^{-1} at 30.0 °C, I = 0.14 M, from ref 2. [e] No inner-sphere product is observed; the reaction proceeds exclusively by the outer-sphere route. [f] 25.0 °C, 0.10 M NaCl media, from ref 28. Compare with 63 M^{-1} s^{-1} at 25.0 °C, 0.20 M NaCl media, from the same source, and 35 ± 2 M^{-1} s^{-1} in 0.1 M NaCl at 25 °C from ref 32. [g] Reference 33.

Results

(a) Reaction Products. The dominant oxidized product in the oxidation of $[Co(en)_3]^{2+}$ by all the oxidants used in this study under conditions of high [en] (0.25 M) is $[Co(en)_3]^{3+}$ as noted previously.[6] For $[Co(gly)(ox)_2]^{2-}$, *cis*-β-[Co(edda)(ox)]⁻, and C_1-*cis*(*N*)-$[Co(gly)_2(ox)]^-$ as oxidants the stoichiometries are 1:0.94, 1:0.94, and 1:0.98, respectively, anticipated for an outer-sphere single-electron-transfer process. However, for *cis*-α-[Co(edda)(ox)]⁻, C_2-*cis*(*N*)-$[Co(gly)_2(ox)]^-$, *trans*(*N*)-$[Co(gly)_2(ox)]^-$, and $[Co(en)(ox)_2]^-$ as oxidants significantly less $[Co(en)_3]^{3+}$ is recovered, with stoichiometries of 1:0.80, 1:0.71, 1:0.77, and 1:0.72 respectively. The remainder of the oxidized product is $[Co(en)_2(ox)]^+$, which can be recovered quantitatively in all the reactions involving the oxalato complexes as [en] is lowered to concentrations where $[Co(en)_2]^{2+}$ is the dominant form of the reductant, Table I.

(b) Kinetics and Mechanisms. The rates of reduction of $[Co(gly)(ox)_2]^{2-}$, [Co(edta)]⁻, *cis*-α-[Co(edda)(ox)]⁻, *cis*-β-[Co(edda)(ox)]⁻, C_1-*cis*(*N*)-$[Co(gly)_2(ox)]^-$, C_2-*cis*(*N*)-$[Co(gly)_2(ox)]^-$, *trans*(*N*)-$[Co(gly)_2(ox)]^-$, and $[Co(en)(ox)_2]^-$ by cobalt(II) in solutions of 1,2-diaminoethane were examined under pseudo-first-order conditions with an excess of reductant at 25.0 °C and 0.10 M ionic strength. Pseudo-first-order rate constants, k_{obsd}, show a first-order dependence on the oxidant concentration and are collected in Table SI. At [en] sufficient to ensure >99% formation of $[Co(en)_3]^{2+}$ where the dominant product is $[Co(en)_3]^{3+}$, plots of k_{obsd} against $[[Co(en)_3]^{2+}]$ are linear with negligible intercepts, and second-order rate constants, k_{os}, are collected in Table II. At lower [en], where significant amounts of $[Co(en)_2]^{2+}$ are in rapid equilibrium with $[Co(en)_3]^{2+}$, eq 1, the reaction rates increase, coincident with the formation of $[Co(en)_2(ox)]^+$ as reaction product.

$$[Co(en)_2]^{2+} + en \overset{K_3}{\rightleftharpoons} [Co(en)_3]^{2+} \qquad K_3 = 2000\ M^{-1} \quad (1)$$

The rate acceleration and the change in reaction products may be understood in terms of a mechanism involving two competing pathways. In one pathway $[Co(en)_3]^{2+}$ is an outer-sphere reductant and in the other $[Co(en)_2]^{2+}$ is an inner-sphere reductant as shown in eqs 2 and 3 for $[Co(en)(ox)_2]^-$ as oxidant. Similar

$$[Co(en)_2]^{2+} + [Co(en)(ox)_2]^- \xrightarrow{k_{is}} [Co(en)_2(ox)]^+ + [Co(en)(ox)] \quad (2)$$

$$[Co(en)_3]^{2+} + [Co(en)(ox)_2]^- \xrightarrow{k_{os}} [Co(en)_3]^{3+} + [Co(en)(ox)_2]^{2-} \quad (3)$$

schemes apply for the other oxidants. The data were fit by an iterative least-squares procedure to eq 4, where k_{os} is the second-

$$k_{obsd} = k_{os}[[Co(en)_3]^{2+}] + k_{is}[[Co(en)_2]^{2+}] \quad (4)$$

order rate constant for outer-sphere reduction by $[Co(en)_3]^{2+}$, and k_{is} is the second-order rate constant for inner-sphere reduction by $[Co(en)_2]^{2+}$. Values of k_{is} are given in Table II. Extensive concentration dependence studies involving $[Co(en)_2]^{2+}$ are not possible due to uncertainties in the distribution of the different forms of the reductant.

The kinetics of the outer-sphere reduction of C_1-*cis*(*N*)- and C_2-*cis*(*N*)-$[Co(gly)_2(ox)]^-$ were also examined in D_2O and pseudo-first-order rate constants are collected in Table SI. Second-order rate constants were calculated to be 1.08 ± 0.05 M^{-1} s^{-1} for the C_1-cis(N) isomer and 0.27 ± 0.01 M^{-1} s^{-1} for the C_2-cis(N) isomer at 25.0 °C and 0.10 M ionic strength (KCl). The solvent isotope effect, $k_{os}(H_2O)/k_{os}(D_2O)$, is calculated to be 1.39 for the C_1-cis(N) isomer and 1.63 for the C_2-cis(N) isomer.

Rates of reduction of the complexes by $[Cr(bpy)_3]^{2+}$ were examined spectrophotometrically at 467 nm under pseudo-first-order conditions with an excess of oxidant at 0.10 M ionic strength. Pseudo-first-order rate constants are reported in Table SII. For $[Co(ox)_3]^{3-}$ and $[Co(gly)(ox)_2]^{2-}$ the reaction rates exceed the upper limit of the stopped-flow technique and are not reported. For the other oxidants, the reaction rates are first order in both reagents, and second-order rate constants are presented in Table II. Pseudo-first-order rate constants for these reactions are faster than the expected rate of dissociation[30] of bpy from $[Cr(bpy)_3]^{2+}$ under the reaction conditions; this leads to the assertion that these reactions are outer-sphere in nature.

(c) Stereoselectivity. Stereoselectivities for the outer-sphere electron transfer reaction of seven of the oxidants with $[Co(en)_3]^{3+}$

(30) Blinn, E. L.; Wilkins, R. G. *Inorg. Chem.* **1976**, *15*, 2952.
(31) Lannon, A. M.; Lappin, A. G.; Segal, M. G. *Inorg. Chem.* **1984**, *23*, 4167–4170.
(32) Beattie, J. K.; Binstead, R. A.; Broccardo, M. *Inorg. Chem.* **1978**, *17*, 1822–1826.
(33) Dwyer, F. P.; Sargeson, A. M. *J. Phys. Chem.* **1961**, *65*, 1892.

Table III. Stereoselectivities (% Enantiomeric Excess) for Reaction of a Series of Oxidants with $[Co(en)_3]^{2+}$ and $[Co(en)_2]^{2+}$ at 25.0 °C and 0.10 M Ionic Strength[a]

	reductant		
oxidant	$[Co(en)_3]^{2+}$	$[Co(en)_2]^{2+}$	IP[b]
Δ-$[Co(ox)_3]^{3-}$	10.1(1) ΔΛ,[c] 9.0(1.4) ΔΛ[d]	1.5(1) ΔΔ[d]	ΔΛ[d]
Δ-$[Co(gly)(ox)_2]^{2-}$	9.0(1) ΔΛ[c]	0.60(3) ΔΔ	ΔΛ[e–g]
Δ-$[Co(edta)]^-$	9.7(1) ΔΛ,[c] 10.8(5) ΔΛ[h]		ΔΛ[f–h]
Δ-*cis*-β-$[Co(edda)(ox)]^-$	8.3(1) ΔΛ	0.5(1) ΔΔ	ΔΛ[f,j]
Δ-C_1-*cis*(*N*)-$[Co(gly)_2(ox)]^-$	9.4(1) ΔΛ,[c] 11.1(1) ΔΛ[k]	1.41(10) ΔΛ	ΔΛ[f,j]
Δ-*cis*-α-$[Co(edda)(ox)]^-$	1.8(1) ΔΛ	3.0(1) ΔΔ	ΔΔ[j]
Δ-C_2-*cis*(*N*)-$[Co(gly)_2(ox)]^-$	2.1(1) ΔΛ,[c] 2.3(1) ΔΛ[k]	2.54(12) ΔΔ	ΔΔ[j]
Δ-*trans*(*N*)-$[Co(gly)_2(ox)]^-$	0.5(1) ΔΛ[c]	6.47(10) ΔΛ	ΔΔ[j]
Δ-$[Co(en)(ox)_2]^-$	3.6(1) ΔΛ[c]	0.80(2) ΔΛ	ΔΔ[g]

[a] Numbers in parentheses indicate error in the last significant figure(s). [b] Ion-pairing selectivity of the oxidant with optically active $[Co(en)_3]^{3+}$. [c] Reference 6. [d] Reference 4. [e] Reference 8. [f] Reference 9. [g] Reference 11. [h] Reference 3. [j] Reference 10. [k] In D_2O.

have been reported previously[6] and are summarized together with results from the present study in Table III. In each case the sense of the stereoselectivity is ΔΛ, although the extent of the chiral induction varies considerably. For C_1-*cis*(*N*)- and C_2-*cis*(*N*)-$[Co(gly)_2(ox)]^-$ there is little change in the stereoselectivity when D_2O is used as a solvent instead of water. The inner-sphere stereoselectivities are also listed in Table III and show both ΔΔ and ΔΛ sense depending on the oxidant.

(d) ^{1}H Relaxation Studies. Proton NMR relaxation experiments in the presence of paramagnetic ions have provided useful information on the structures of labile ion pairs in solution.[34] Interactions of $[Cr(en)_3]^{3+}$, a paramagnetic analogue of $[Co(en)_3]^{2+}$, with the diamagnetic complexes cis-α-$[Co(edda)(ox)]^-$ and cis-β-$[Co(edda)(ox)]^-$ were investigated at 0.10 M ionic strength. These complexes were selected because they have sufficient unique ^{1}H environments to allow evaluation of structural information for the ion pair by the NMR method. Some studies were also carried out with C_1-*cis*(*N*)- and C_2-*cis*(*N*)-$[Co(gly)_2(ox)]^-$, and with C_1-*cis*(*N*)- and C_2-*cis*(*N*)-$[Co(aib)_2(ox)]^-$ (aib = aminoisobutyrate(1–)) at 0.10 M ionic strength, and while there is qualitative agreement between the experiments, these later studies do not allow unique determinations of structure.[35] With *cis*-β-$[Co(edda)(ox)]^-$ there is a complication relating to the presence of diastereomers[26] Λ(*RS*), Λ(*RR*), Δ(*SR*), and Δ(*SS*) which differ in the absolute configuration at the nitrogen bound to the in-plane carboxylate group. The previous assignment noted a single diastereomer, but in the present work, both diastereomers are present in the ratio 1:1.5. The dominant isomer is assigned the Λ(*RS*)/Δ(*SR*) configuration, and the assignments of the ^{1}H NMR peaks for the complexes in Figure 2 are given in Table IV.[24,25] Structural data are not available for the complexes, and representations of the ^{1}H positions for these complexes were generated by comparisons with crystallographic data for the structurally related $[Co(edta)]^-$ complex.[36]

In a structured ion pair with $[Cr(en)_3]^{3+}$, the spin–lattice relaxation times (T_1) for the complexes decrease according to eq 5, where M_{diam} is the mole fraction of the diamagnetic complex

$$(1/T_1)_{obsd} = M_{diam}(1/T_1)_{diam} + M_{para}(1/T_1)_{para} + R_{unstruct}[[Cr(en)_3]^{3+}] \quad (5)$$

free in solution, M_{para} is the mole fraction in the structured ion pair, $(1/T_1)_{diam}$ is the relaxation rate in the absence of the

(34) Marusak, R. A.; Lappin, A. G. *J. Phys. Chem.* **1989**, *93*, 6856–6859.
(35) Warren, R. M. L.; Lappin, A. G. Unpublished observations.
(36) Tatehata, A.; Haller, K. J.; Warren, R. M. L.; Lappin, A. G. Manuscript in preparation.

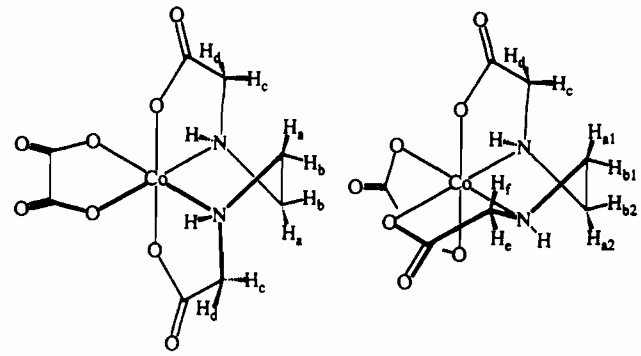

Figure 2. Structures of *cis*-α-$[Co(edda)(ox)]^-$ and *cis*-β-$[Co(edda)(ox)]^-$ illustrating the proton labeling scheme for Table IV.

Table IV. ^{1}H NMR Assignments and Relaxivities from Plots of $(1/T_1)$ against $[[Cr(en)_3]^{3+}]$ for the Protons in *cis*-α-$[Co(edda)(ox)]^-$ and *cis*-β-$[Co(edda)(ox)]^-$ at 25 ± 0.5 °C and 0.10 M Ionic Strength

cis-α-$[Co(edda)(ox)]^-$

H_a	3.30 ppm	2680 M^{-1} s^{-1}	H_b	2.79 ppm	1560 M^{-1} s^{-1}
H_c	3.38 ppm	2550 M^{-1} s^{-1}	H_d	4.28 ppm	5040 M^{-1} s^{-1}

cis-β-$[Co(edda)(ox)]^-$

H_{a1}	2.93 ppm	4310 M^{-1} s^{-1}	H_{b1}	2.73 ppm	2500 M^{-1} s^{-1}
H_{a2}	3.32 ppm	3480 M^{-1} s^{-1}	H_c	3.11 ppm	overlap with H_{b2}
H_d	3.93 ppm	9890 M^{-1} s^{-1}	H_e, H_f	3.56 ppm	7810 M^{-1} s^{-1}

paramagnetic ion, $(1/T_1)_{para}$ is the relaxation rate in the isolated structured ion pair, and $R_{unstruct}$ is the relaxivity due to unstructured paramagnetic interactions. When the diamagnetic complex is present in large excess, the term M_{para} may be approximated by eq 6, where K_0 is the macroscopic equilibrium constant for the

$$M_{para}(1/T_1)_{para} = \frac{K_0}{1 + K_0[Co(III)]_T}(1/T_1)_{para}[[Cr(en)_3]^{3+}]_T = R_{struct}[[Cr(en)_3]^{3+}]_T \quad (6)$$

structured ion pair, and the subscript T represents total concentration. Both structured (R_{struct}) and unstructured ($R_{unstruct}$) contributions to the relaxivity show a linear dependence on $[[Cr(en)_3]^{3+}]_T$. Separation of these contributions may be achieved by least-squares optimization of the Solomon–Bloembergen correlation[37,38] between R_{struct} and $(1/N)\Sigma(r_i)^{-6}$ where r_i is the distance between the paramagnetic center and the *i*th equivalent proton and N is the number of equivalent proton environments in the complex. For *cis*-β-$[Co(edda)(ox)]^-$, there are eight unique proton environments; however two are coincident and two overlap to such an extent that independent T_1 values cannot be obtained. Although there are some ambiguities about the conformation of the chelate rings, a fit to the remaining five values yields a local optimized fit with a Co–Cr distance of 5.3 Å. The intercept, representing unstructured interactions is 560 M^{-1} s^{-1}. Interestingly neither intercept nor the direction of the Cr–Co vector varies significantly with the Cr–Co distance. The paramagnetic center is located on the pseudo-C_3 face of the complex but tilted toward the pseudo-C_2 axis, Figure 3. For *cis*-α-$[Co(edda)(ox)]^-$ there are only four unique environments, and while excellent fits are obtained, the function in eq 6 cannot be minimized at chemically reasonable distances with a positive intercept. This is most likely the result of ambiguities in the conformationally more flexible 1,2-diaminoethane backbone. However, a good fit was obtained by holding the intercept and Co–Cr distance close to the values obtained for the *cis*-β-$[Co(edda)(ox)]^-$ isomer on the assumption that unstructured interactions with both cobalt(III) isomers will

(37) Solomon, I. *Phys. Rev.* **1955**, *99*, 559–565.
(38) Bloembergen, N. *J. Chem. Phys.* **1957**, *27*, 572–573.

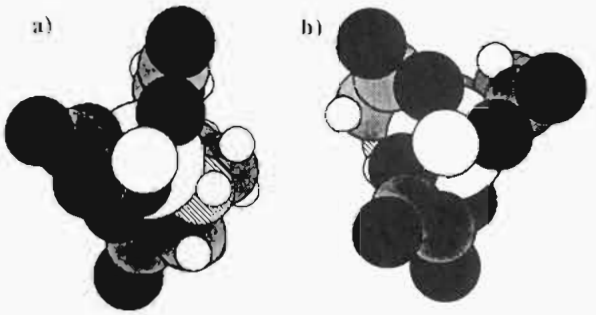

Figure 3. Positions of the paramagnetic center calculated from NMR relaxivity studies with respect to (a) *cis*-α-[Co(edda)(ox)]$^-$ and (b) *cis*-β-[Co(edda)(ox)]$^-$. The view in both cases is along the Cr–Co axis. Black spheres represent O, gray represent C, and striped represent N.

be similar. The position of the paramagnetic center lies on an edge of the complex close to oxalate, Figure 3.

Discussion

All the reactions of the oxalato complexes examined in this study show behavior similar to that of $[Co(ox)_3]^{3-}$ where electron transfer takes place by two competing pathways, an outer-sphere pathway leading to $[Co(en)_3]^{3+}$ and an inner-sphere pathway with a doubly bridging oxalate group leading to $[Co(en)_2(ox)]^+$. It must be noted that outer-sphere oxidation of $[Co(en)_2(ox)]$ provides an alternative pathway for formation of $[Co(en)_2(ox)]^+$. However ^{13}C-labeling studies with $[Co(ox)_3]^{3-}$ as oxidant have shown that more than 98% of the oxalate in the product originates with the $[Co(ox)_3]^{3-}$, suggesting that the inner-sphere pathway is the correct assignment.[4] The absence of a second reaction pathway for $[Co(edta)]^-$, which has no oxalate group, lends credence to the doubly bridged inner-sphere mechanism.

The second-order rate constants for the outer-sphere oxidation of $[Co(en)_3]^{2+}$ are presented in Table II. Reduction potential data are not available for most of the oxidants under discussion although it is generally recognized that reduction potentials decrease as carboxylate oxygen donor ligands are replaced by amine nitrogen ligands. The extreme examples are $[Co(ox)_3]^{3-/4-}$ with $E^\circ = 0.57$ V[39] and $[Co(en)_3]^{3+/2+}$ with $E^\circ = -0.18$ V.[40] Various estimates of reduction potentials for intermediate members of the series have been made,[41] but apart from $[Co(edta)]^-$ with $E^\circ = 0.37$ V,[42] the values are not reliable since the couples are irreversible. The rates of the outer-sphere reactions parallel the expected changes in reduction potential, perhaps suggesting that the self-exchange rates for the complexes are uniformly slow.

Comparative Marcus theory predicts that the rates of outer-sphere reduction by $[Co(en)_3]^{2+}$ should show a linear free energy correlation with the rates of reduction by $[Cr(bpy)_3]^{2+}$. A plot of log k_{os} against log k_{Cr} is shown in Figure 4, and the correlation is fair, eq 7, with slope 1.24 ± 0.14 slightly larger than the value

$$\log k_{os} = -6.85 + 1.24 \log k_{Cr} \qquad (7)$$

of unity which is predicted by the Marcus relationship. Bearing in mind that the radii of the two reductants differ and that the charges on the oxidants vary from −1 to +3, the correlation is not unacceptable.

However, closer inspection of the data, Table II, reveals that for the anionic complexes, there are two distinct reactivity domains with $k_{Cr}/k_{os} \approx 5 \times 10^5$ and $\approx 1 \times 10^5$, shown by the solid lines of unit slope[43] in Figure 4. The set with the smaller ratio consists exclusively of the complexes which posses the unhindered C_3 motif,

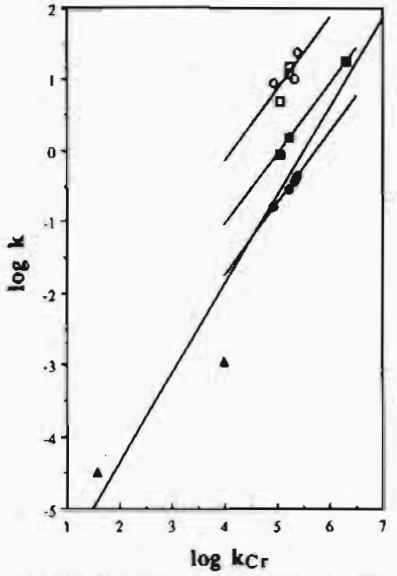

Figure 4. Linear free energy correlation between the rates of reduction of the cobalt(III) complexes by $[Co(en)_3]^{2+}$, closed symbols, and $[Co(en)_2]^{2+}$, open symbols, with the corresponding rates of reduction by $[Cr(bpy)_3]^{2+}$. Squares represent anionic complexes with the C_3 motif, circles represent anionic complexes lacking the C_3 motif, and triangles represent cationic complexes. All data were obtained at 25.0 °C and 0.10 M ionic strength.

whereas the set with the larger ratio consists exclusively of complexes possessing the hindered C_3 motif. The difference in activation free energy corresponds to ≈4 kJ mol^{-1} and is ascribed to stabilization of the precursor assembly by an increase in hydrogen bonding. The magnitude of the increased stabilization corresponds to a fraction of the strength of a hydrogen bond. Presumably there is a compensating mechanism where some weakening of existing hydrogen bonds is compensated by the formation of an additional interaction. Solvent isotope effects, $k_{os}(H_2O)/k_{os}(D_2O)$, measured for reactions of members of the two sets of compounds, C_1-*cis*(*N*)- and C_2-*cis*(*N*)-$[Co(gly)_2(ox)]^-$, are 1.39 and 1.63, respectively and are comparable with solvent isotope effects in other outer-sphere electron transfer reactions. This suggests that the solvent has no special role in the rate limiting step.

In support of this interpretation that the differences in reactivity arise from differences in ion-pairing between the reactants which precede the electron-transfer step, it should be noted that the ion association constants for interactions between the oxidants and $[Co(en)_3]^{3+}$ are an order of magnitude larger for complexes which have the C_3 motif than those which do not.[10,11] The NMR relaxation studies with *cis*-α-[Co(edda)(ox)]$^-$ and *cis*-β-[Co(edda)(ox)]$^-$, where only the latter isomer has the C_3 motif, yield good representations of relative orientations of the anionic complexes with $[Cr(en)_3]^{3+}$. These studies tend to support the hypothesis that the interactions are quite different. For *cis*-β-[Co(edda)(ox)]$^-$, the axis of approach of the paramagnetic center lies close to the pseudo-C_3 axis of the complex and would allow formation of a triply hydrogen-bonded ion pair involving amine protons on the C_3 face of $[Cr(en)_3]^{3+}$. Remarkably, the orientation of the paramagnetic center is almost identical to that found with $[Co(edta)]^-$.[34] A strong C_3–C_3 hydrogen bonding interaction has been shown in an X-ray structure determination of $[Co(en)_3][Rh(ox)_3]$, where the Co–Rh distance is around 5 Å.[44] For *cis*-α-[Co(edda)(ox)]$^-$ the relaxivities are smaller, consistent with a weaker interaction, and the paramagnetic center

(39) Hin-Fat, L.; Higginson, W. C. E. *J. Chem. Soc. A* **1967**, 298–301.
(40) Creaser, I. I.; Sargeson, A. M.; Zanella, A. W. *Inorg. Chem.* **1983**, *22*, 4022–4029.
(41) Ohashi, K. *Bull. Chem. Soc. Jpn.* **1972**, *45*, 3093–3095.
(42) Ogino, H.; Ogino, K. *Inorg. Chem.* **1983**, *22*, 2208–2211.

(43) Least squares analysis of the data gives the following fits, with errors in parentheses. Overall: low $k_{os} = -6.85(71) + 1.24(14) \log k_{Cr}$. C_3 motif present: log $k_{os} = -5.24(17) + 1.03(3) \log k_{Cr}$. C_3 motif absent: log $k_{os} = -5.51(32) + 0.95(6) \log k_{Cr}$.

(44) Kuroda, R. *Inorg. Chem.* **1991**, *30*, 4954–4959.

is positioned above the oxalate ligand in line with one of the carboxylate groups of the edda ligand. There is an equivalent point related by the C_2 axis. Again it is of considerable interest to note that a similar orientation for $[Co(en)_3]^{3+}$ relative to $[Co(en)(ox)_2]^-$ is found in the X-ray structure of Δ-$[Co(en)_3]\Delta$-$[Co(en)(ox)_2]I_2 \cdot H_2O$ where the Co-Co distance is 5.7 Å.[36] There are hydrogen bonds between amine protons on $[Co(en)_3]^{3+}$ and terminal and metal-bound oxygens of a single carboxylate in $[Co(en)(ox)_2]^-$. This carboxylate corresponds to the carboxylate group on the edda ligand of *cis*-α-$[Co(edda)(ox)]^-$.

While it must be remembered that the NMR relaxation data arise from an assembly of microstructures rather than a single structure, it is clear that there are preferred orientations and that these orientations differ considerably for the two isomers. It can be argued that the differences in the electron-transfer rates are the result of different probabilities for electron transfer for the different orientations. Indeed, there are clear indications in the reaction of $[Co(ox)_3]^{3-}$ with $[Co(phen)_3]^{2+}$ that such effects are important.[45] In the present study it is noted that ion pair formation between $[Co(en)_3]^{3+}$ and anionic complexes without the C_3 motif exhibits a stereoselectivity in which the $\Delta\Delta$ pair is preferred, contrasting with the electron transfer stereoselectivities where a $\Delta\Lambda$ preference is found. It may be that in this instance the preferred ion pair orientation does not allow facile electron transfer. On the other hand the C_3 motif promotes a $\Delta\Lambda$ interaction both in the ion pair with $[Co(en)_3]^{3+}$ and in electron transfer with $[Co(en)_3]^{2+}$. The change in stereoselectivity which results from inclusion of the C_3 motif corresponds to $\approx$0.4 kJ mol^{-1}, about 10% of the change in activation energy.

Rates for the inner-sphere electron-transfer pathway are faster than the corresponding outer-sphere rates despite a thermodynamic disadvantage. The rates show a trend with reduction potential which parallels the rate with $[Cr(bpy)_3]^{2+}$, eq 8, although

$$\log k_{is} = -3.89 + 0.95 \log k_{Cr} \qquad (8)$$

the range of values available is limited. Stereoselectivities for the inner-sphere reaction are presented in Table III. They vary from 6.47% $\Delta\Lambda$ for *trans*(*N*)-$[Co(gly)_2(ox)]^-$ to 3.0% $\Delta\Delta$ for *cis*-α-$[Co(edda)(ox)]^-$. There is an underlying trend with these data which reflects the structures of the oxidant complexes. The ligand donor groups in positions cis to both arms of the bridging oxalate group control the stereoselectivity. Where these are both carboxylate, the stereoselectivity lies between 1.5% and 3.0% $\Delta\Delta$. When one carboxylate and one amine are present, the stereoselectivity lies between 0.5% $\Delta\Delta$ and 1.41% $\Delta\Lambda$, while the two amine groups in *trans*(*N*)-$[Co(gly)_2(ox)]^-$ give 6.47% $\Delta\Lambda$. In the one example, $[Co(gly)(ox)_2]^{2-}$, which has one oxalate group with cis-amine and cis-carboxylate and a second oxalate group with two cis-carboxylate groups, the stereoselectivity is 0.60% $\Delta\Delta$, which does not allow assignment of a preferred bridge. However, hydrogen bonding between the cis-ligand donor groups and the inner-sphere reductant, $[Co(en)_2]^{2+}$, appears to have a controlling influence. Carboxylate groups can form strong hydrogen bonds, but amine groups cannot. Some support for this notion comes from a previous study of inner-sphere stereoselectivity in the reduction of $[Co(ox)_3]^{3-}$ by $[Co(N,N\text{-}Me_2en)_2]^{2+}$ and $[Co(N,N'\text{-}Me_2en)_2]^{2+}$.[46] The $[Co(N,N'\text{-}Me_2en)_2]^{2+}$ is capable of the hydrogen bonding interaction and shows enhanced $\Delta\Delta$ stereoselectivity but with $[Co(N,N\text{-}Me_2en)_2]^{2+}$, the permethylated amines are cis to the bridging oxalate and is incapable of forming hydrogen bonds. The stereoselectivity is 4.3% $\Delta\Lambda$.

In conclusion, variations in oxidant structure have been used to probe the electron transfer reactions of $[Co(en)_3]^{2+}$ and $[Co(en)_2]^{2+}$. For both inner-sphere and outer-sphere pathways, hydrogen bonding has a small but profound effect on the nature of the interaction between the reactants. As a consequence the combination of rate and stereoselectivity data, which reflect the nature of the interaction, provides exquisite detail of the reaction mechanism.

Acknowledgment. The support of the National Science Foundation (Grant No. CHE 90-16682) is gratefully acknowledged.

Supplementary Material Available: Lists of pseudo-first-order rate constants (Tables SI and SII) (9 pages). Ordering information is given on any current masthead page.

(45) Warren, R. M. L.; Lappin, A. G.; Tatehata, A. *Inorg. Chem.* **1992**, *31*, 1566–1574.

(46) Marusak, R. A.; Ivanca, M. A.; Haller, K. J.; Lappin, A. G. *Inorg. Chem.* **1991**, *30*, 618–623.